

THE QUEST FOR THE BEST GRAPHIC EQUALIZER

Juho Liski* and Vesa Välimäki

Aalto University
Acoustics Lab, Dept. of Signal Processing and Acoustics
Espoo, Finland
juho.liski@aalto.fi

ABSTRACT

The design of graphic equalizers has been investigated for decades, but only recently fitting the magnitude response closely enough to the control points has become possible. This paper reviews the development of graphic equalizer design and discusses how to define the target response. Furthermore, it investigates how to find the hardest target gain settings, the definition of the bandwidth of band filters, the estimation of the interaction between the bands, and how the number of iterations improves the design. The main focus is on a recent design principle for the cascade graphic equalizer. This paper extends the design method for the case of third-octave bands, showing how to choose the parameters to obtain good accuracy. The main advantages of the proposed approach are that it keeps the approximation error below 1 dB using only a single second-order IIR filter section per band, and that its design is fast. The remaining challenge is to simplify the design phase so that sufficient accuracy can be obtained without iterations.

1. INTRODUCTION

The design of graphic equalizers (EQ) is surprisingly difficult, and for this reason it has been investigated for decades [1]. The first application of graphic EQs was the enhancement of audio quality in movie systems in the 1950s [2, 1]. In the early years, graphic EQs were analog, but since the 1980s digital designs have been proposed [2, 3, 4, 5]. The graphic EQ has become one of the standard tools in music production [2, 6] and in audio systems [7, 8, 9, 10].

This paper reviews the development of graphic EQs, investigates the graphic EQ design problem, and discusses the recent efforts to improve and simplify the design of digital graphic EQs. Section 2 of this paper reviews the development of graphic equalizers. In Section 3, we first tackle the definition of target response and how to evaluate the accuracy of the design. Section 4 elaborates further on a recently proposed cascade octave graphic EQ design [11], trying to understand whether there are ways to improve it. Furthermore, in Section 5, we expand the proposed cascade design for the third-octave case, which is another popular and useful configuration. Section 6 concludes this paper and shows avenues for future research in this topic.

2. HISTORICAL DEVELOPMENTS

The graphic EQ design problem is simple: to fit the magnitude response of a digital filter through control points, which define the gain at several predefined frequency points. These are often called

the command gains. It was quickly understood that fitting the magnitude response of an EQ through the command points, which are usually spaced logarithmically in frequency is very difficult. Only recent digital design methods have achieved sufficient accuracy for hi-fi audio [12, 13, 1].

One straightforward method is to fit the response of a finite impulse response (FIR) filter to the command point data using interpolation and to apply the inverse discrete Fourier transform to obtain the FIR filter coefficients [14, 15]. However, the frequency division in graphic EQs is usually logarithmic, such as octaves, and the use of an FIR filter leads to complications at low frequencies: the impulse response associated with a sharp change in a low-frequency band becomes very long [15]. One idea to reduce this complication is using a multirate system to optimally down-sample the long filters at low frequencies [16, 17]. Alternatively, frequency warping can be used to shorten the filter at low frequencies, but still, FIR graphic EQs are currently more costly to implement than infinite impulse response (IIR) graphic EQs [18].

During the analog era, most graphic EQs were based on the parallel structure, which refers to a bank of bandpass filters all of which receive the same input signal [19, 5, 20, 21, 12, 1]. The outputs of the bandpass filters were amplified according to the command gain of that band, and then combined (summed). Such structures suffered from complications due to the interference of the magnitude and phase responses of the neighboring bandpass filters. These often led to notches in the transition region from one band to another, or accumulation of gain in some bands due to leakage from neighboring bands. Early digital graphic EQs inherited the parallel structure from the analog world [5]. A few years ago, Rämö *et al.* showed how a graphic EQ can be designed accurately using a parallel filter, which is based on least-squares (LS) optimization of a bank of IIR filters having fixed poles [12].

As an alternative, the cascade structure has been considered for graphic EQs [19, 22, 23, 24, 1]. Traditional parametric EQ filters can be used as building blocks of a cascade graphic EQ [22, 25, 13]. It is well known in digital signal processing that the same transfer functions can be implemented using either a parallel or a cascade filter [26]. However, the design of the filter parameter values for these structures can be very different. The main reason for this is that considering the phase response of the band filters is unnecessary in the case of the cascade structure [1, 11]. However, in the case of the parallel structure, the phase response of each band filter is critical, as in the end the output signals of all band filters are combined.

Cascade graphic EQs suffer from similar interference from neighboring band filters as parallel EQs [1]. Some solutions to this problem include variable-Q designs, which change the bandwidth of the band filter according to the gain [27], and higher-order band filters, which improve the summation of the neighboring bands

* J. Liski is supported by the Aalto ELEC Doctoral School. The work was partially funded by Nokia Technologies (Aalto project number 410642).

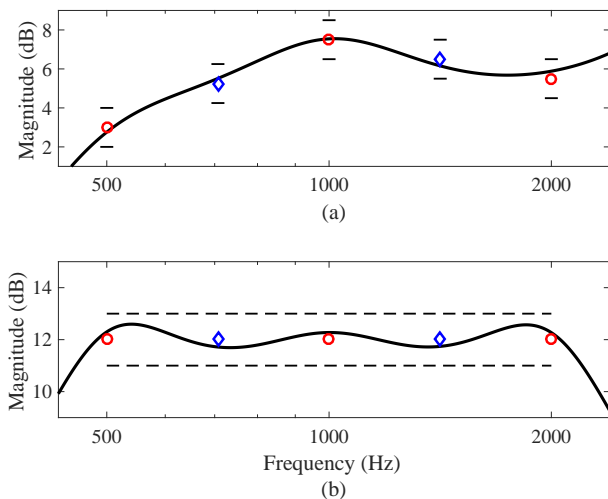


Figure 1: Definition of the ± 1 -dB error limits in the case of (a) different and (b) same neighboring command gains (red circles). In both figures, the blue diamonds indicate the extra points midway between each command point.

at the cost of increased computational complexity [28, 23, 24]. Our recent work showed that in the case of the octave cascade graphic EQ, a sufficiently accurate design can be obtained using a fairly simple design, which involves an unusual definition of filter bandwidth and the LS optimization with one iteration [11]. Additionally, the new cascade filter can be implemented with fewer second-order sections than the best parallel graphic EQ, which requires twice as many biquad filter sections as there are command points. It now seems clear that the best graphic EQ design must be based on the cascading of second-order band filters.

3. DEFINING THE BEST OCTAVE GRAPHIC EQ

There are multiple ways to compare different EQ designs. Commonly, the maximum error, the computational cost of the implementation, and the complexity of the design are used as criteria [12]. This section discusses ways to define the target response and how to test graphic EQ designs. Both aspects affect the evaluation of the maximum error.

3.1. Target Response

Obviously, the magnitude response of a graphic EQ should match the command gains at the control frequencies very closely. In hi-fi audio, a 1-dB accuracy requirement is typical at those points [23, 12, 1]. The error function used is usually the magnitude frequency response error in dB.

However, how to define the target response between the command points is less obvious. Smooth and monotonous transitions from one command point to another are usually desirable, since in practice a large increase or decrease in the filter gain between the command points is not what an audio engineer expects from a graphic EQ. Various interpolation methods have been suggested for producing a virtually continuous target magnitude response from command gain data [12, 29]. Some design methods require such a high-resolution target response.

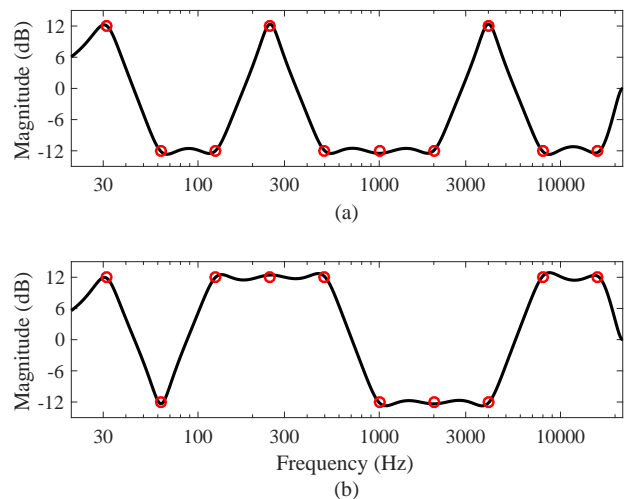


Figure 2: Worst-case command gain (red circles) settings (a) reported by Oliver and Jot for their design [13] and (b) observed in this work for the new cascade design [11]. The black curve is the magnitude response obtained with the proposed design.

We have observed that for a cascade octave graphic EQ having low-order band filters, such as second-order IIR filters, interpolating a high-resolution target response is unnecessary, since the band filter’s gain cannot make large deviations between command points. To guarantee a monotonous transition between command points, one option is to simply define one intermediate point between each command point, where the gain error is evaluated, as suggested in [11]. The gain at the intermediate point is determined as the average of the adjacent command gains in dB. The frequency of the intermediate point must be the geometric mean of the neighboring command points. Figure 1 visualizes this error definition. Figure 1(a) shows the ± 1 -dB error limits at three command points and at two intermediate points between them.

Figure 1(b) presents a common special case in which two or more neighboring command gains are equal. In this case, it is meaningful to require the magnitude response to stay within 1 dB from the command gain also at all frequencies between these points.

3.2. Hardest Gain Settings

In a graphic EQ, the gains can usually be adjusted in the range of ± 12 dB [1]. When trying to find the hardest command gain combinations, testing the settings where the gains are set either to $+12$ or -12 dB in order to produce the largest deviations between the bands is natural. Since there are ten bands in an octave EQ and we have two alternatives, we obtain $2^{10} = 1024$ different combinations, or binary settings. These combinations can then easily be tested to find the one producing the largest error.

Figure 2 shows two examples where the gains are selected from the binary cases. Oliver and Jot found that for their proposed design the worst-case gain setting was the one shown in Fig. 2(a) [13]. On the other hand, our previous work found the settings seen in Fig. 2(b) to cause the largest error. Clearly, these two examples have similarities: there are steep transitions between ± 12 dB, but also plateaus, where the EQ has to produce the same gain in multiple adjacent bands. In both cases, the largest error was actually produced at such a plateau, at approximately 1 kHz [13] and

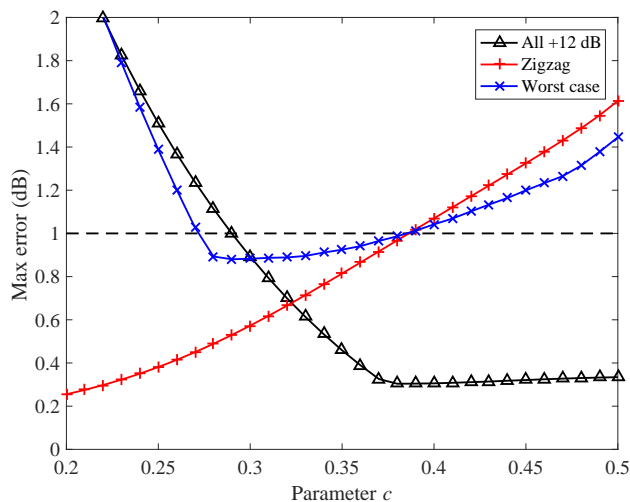


Figure 3: Effect of the value of c on the maximum error in three different command gain settings. The worst case is the one shown in Fig. 2(b). The dashed line indicates the 1-dB error that should not be exceeded.

at 9 kHz [11].

Based on the two cases reviewed above and our own comprehensive testing, we propose that the 1024 hard binary cases should be utilized to test graphic octave EQs in order to reveal the largest approximation error. Note, however, that for the third-octave EQ, there are about 30 command gains, so exhaustive testing of all combinations may not be viable.

4. OCTAVE GRAPHIC EQ DESIGN

Here, a summary of the new cascade graphic EQ design proposed in [11] is presented. The method is based on designs proposed by Abel and Berners [30] and Oliver and Jot [13]: one filter per octave band is used whose interaction with its two neighboring filters at their center frequency is exactly controlled.

The method uses as band filters the following second-order IIR peak/notch filter given by Orfanidis in which the reference gain at dc is set to 1 [31]:

$$H(z) = \frac{1 + G\beta - 2\cos(\omega_c)z^{-1} + (1 - G\beta)z^{-2}}{1 + \beta - 2\cos(\omega_c)z^{-1} + (1 - \beta)z^{-2}}, \quad (1)$$

where G is the linear peak gain, $\omega_c = 2\pi f_c/f_s$ is the normalized center frequency in radians (the ten standard octave frequencies 31.25 Hz, 62.5 Hz, 125 Hz etc. are used), f_s is the sampling frequency, β is defined as

$$\beta = \begin{cases} \tan(B/2), & \text{when } G = 1, \\ \sqrt{\frac{|G_B^2 - 1|}{|G^2 - G_B^2|}} \tan\left(\frac{B}{2}\right) & \text{otherwise,} \end{cases} \quad (2)$$

and G_B is the linear gain at bandwidth $B = 2\pi f_B/f_s$.

In the IIR section defined by (1) and (2), the bandwidth can be selected such that for the m th band filter, a specified dB gain $g_{B,m} = cg_m$ is reached at the neighboring center frequencies. We

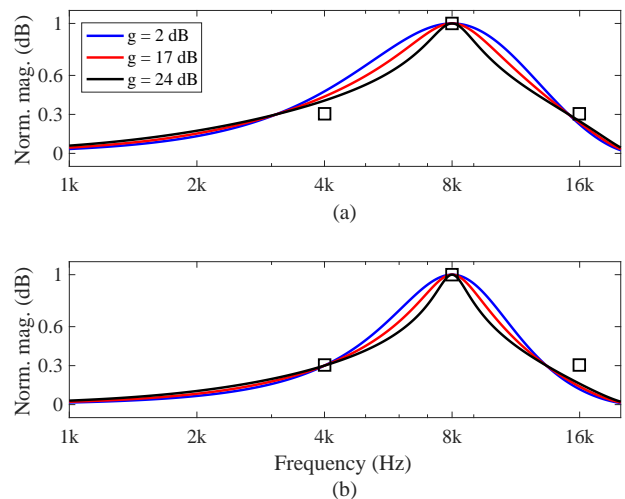


Figure 4: Normalized amplitude responses of the 8-kHz band filter for three different peak gain values: (a) the original bandwidth, which leads to too wide a response (the responses do not cross inside the boxes) and (b) the adjusted bandwidth, which makes the responses cross at the lower neighboring center frequency. The squares indicate the points where the responses should meet.

found that the choice $c = 0.3$ leads to a successful octave graphic EQ design [11]. This is illustrated in Fig. 3, which shows the effect of the parameter c with three different command gain settings. As is seen, the desired accuracy is achieved when c has values between 0.28 and 0.38, and thus $c = 0.3$ can be used. This value of the parameter c leads to an unusual definition of the bandwidth, since traditionally the bandwidth of a resonance is determined as the difference of -3 -dB points on each side of a peak, which refers to 0.7 times the linear gain. However, this non-traditional choice appears to be crucial for accurate automatic design.

The bandwidths is selected as $B_m = 1.5\omega_{c,m}$, which equals the difference between the neighboring upper and lower center frequencies. This way, the behavior of each band filter can be exactly controlled at the center frequencies of both its neighbors. However, at high center frequencies, the bandwidth needs to be adjusted in another way, because the filter response becomes asymmetric.

Figure 4(a) shows examples of the normalized magnitude response of the band filter at 8 kHz for three different gains. The magnitude responses have been normalized on the dB scale by dividing them by their respective dB gain, as suggested in [30]. Without the bandwidth adjustment, the filter responses do not cross at the desired points, i.e., at their center frequency and the two neighboring center frequencies, as seen in Fig. 4(a). This anomaly leads to difficulties in predicting the interaction between neighboring band filters. In the octave design, the asymmetry concerns the three band filters with the highest center frequencies, 4 kHz, 8 kHz, and 16 kHz. Their bandwidth is set so that the $0.3g_m$ point occurs at the lower neighboring center frequency (but not at the higher one), as shown in Fig. 4(b). This leads to bandwidth values $f_{B,8} = 5580$ Hz, $f_{B,9} = 9360$ Hz, and $f_{B,10} = 12160$ Hz instead of 6000 Hz, 12000 Hz, and 24000 Hz, respectively.

The resulting filter-response shapes for all band filters of the cascade octave graphic EQ are shown in Fig. 5, where the responses are seen to meet at all the desired frequency points (the

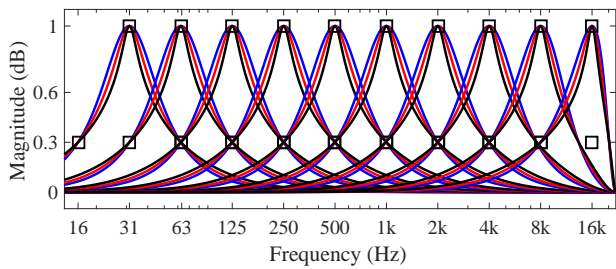


Figure 5: Normalized amplitude responses of all the band filters, which have gains of 0.3 times its peak gain in dB at the neighboring center frequencies, with different peak gain values: 2 dB (blue), 17 dB (red), and 24 dB (black).

squares) except for the three highest filters whose responses do not cross at their higher neighboring frequency. Additionally, Fig. 5 demonstrates the self-similarity of the band filters. Three responses are plotted at each band with different peak gains. Due to the similar shape of each normalized response, the samples taken from the dB amplitude responses can be used as a basis function in order to control the interaction of the band filters at the selected frequencies [30, 13, 11]. The normalized dB amplitude responses of the filters are stored in an interaction matrix \mathbf{B} .

The octave design uses 19 design points [11] instead of ten, as suggested by Oliver and Jot [13]. These 19 points include the filter center frequencies and the geometric mean of these values between them. This decreases the error and thus improves the behavior of the EQ between the command points. With ten octave bands and 19 design frequencies we obtain a 19-by-10 interaction matrix, which is visualized in Fig. 6. The filters for the interaction matrix are designed with (1) and (2) using a prototype dB-gain g_p , which in this case is 17 dB. The values inserted into the interaction matrix represent the magnitude response divided by g_p at the command points and the intermediate points. As is seen in Fig. 6, the diagonal values of the interaction matrix are 1 dB, representing the filter center frequencies, and the other stems indicate the relative effect of each band filter at the other design points.

The interaction matrix is utilized to determine the optimal dB gain for each filter in the LS sense by solving its inverse matrix [32]. However, since the method uses a non-square matrix, the pseudoinverse of the interaction matrix \mathbf{B}^+ is necessary to obtain the optimal solution [32]. The filter gains \mathbf{g} are then obtained as

$$\mathbf{g} = \mathbf{B}^+ \mathbf{t}_1 = (\mathbf{B}^T \mathbf{B})^{-1} \mathbf{B}^T \mathbf{t}_1, \quad (3)$$

where \mathbf{t}_1 is a vector with 19 elements containing the original target dB-gain values in odd rows and their linearly interpolated intermediate values in even rows.

Finally, to achieve the desired accuracy of 1 dB, one iteration step is required, because the shape of the basis functions vary slightly with the filter gains [11]. A new interaction matrix \mathbf{B}_1 is formed with the gains \mathbf{g} obtained from (3) instead of the prototype gain g_p , and new filter gains are calculated similarly to (3). The effect of iteration steps is shown in Fig. 7. Figure 7(a) shows the largest filter gain change in dB as a function of the number of iteration steps. The hardest command gain setting shown in Fig. 2(b) has been used as the target. The first iteration step is seen to cause gain changes up to approximately 0.4 dB when compared to the non-iterative version, whereas the second step has an effect of approximately 0.05 dB or less. After the third iteration step the gains

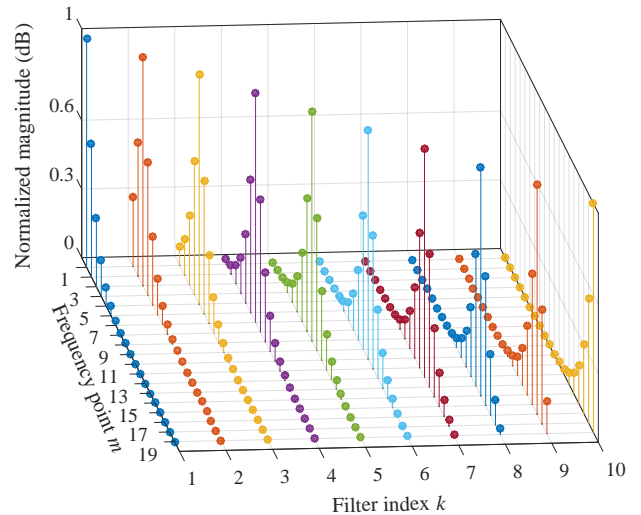


Figure 6: A 19-by-10 interaction matrix containing the normalized leakage of each band filter to the other frequency points.

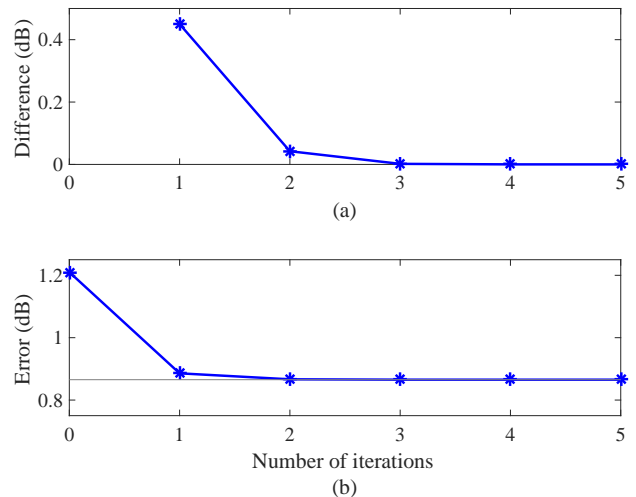


Figure 7: (a) Maximum difference in filter gains between the iteration rounds, and (b) maximum error after each iteration for the hardest command gain setting of the octave graphic EQ, cf. 2(b).

practically do not change at all.

On the other hand, Fig. 7(b) shows the maximum approximation error in each case. As is seen, the acceptable error of less than 1 dB is achieved with one iteration, and the second iteration decreases the error very slightly. After that, the error saturates at 0.87 dB and further iteration steps have practically no effect. Similar error behavior is observed with other tested target responses. Thus, it is safe to assume that iterating the interaction matrix once suffices, and that further iterations are superfluous.

5. THIRD-OCTAVE DESIGN

In this section we devise a third-octave cascade graphic EQ design based on the octave version. One second-order peak/notch filter of the form (1) is used for each band. Also, an interaction matrix

Table 1: Center frequencies and bandwidths for the 31 filters of the third-octave graphic equalizer. The adjusted bandwidths of the six highest band filters are shown in italics.

	1	2	3	4	5	6	7	8	9	10	11
f_c (Hz)	19.69	24.80	31.25	39.37	49.61	62.50	78.75	99.21	125.0	157.5	198.4
f_B (Hz)	9.178	11.56	14.57	18.36	23.13	29.14	36.71	46.25	58.28	73.43	92.51
	12	13	14	15	16	17	18	19	20	21	22
f_c (Hz)	250.0	315.0	396.9	500.0	630.0	793.7	1000	1260	1587	2000	2520
f_B (Hz)	116.6	146.9	185.0	233.1	293.7	370.0	466.2	587.4	740.1	932.4	1175
	23	24	25	26	27	28	29	30	31		
f_c (Hz)	3175	4000	5040	6350	8000	10080	12700	16000	20160		
f_B (Hz)	1480	1865	2350	<i>2846</i>	<i>3502</i>	<i>4253</i>	<i>5038</i>	<i>5689</i>	<i>5573</i>		

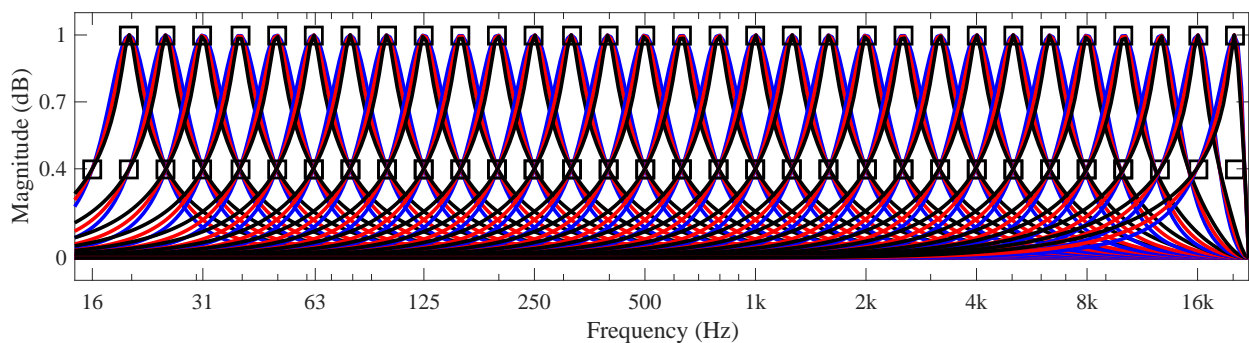


Figure 8: Normalized amplitude responses of all third-octave band filters with three different peak gains, as in Fig. 5. The filter gain at the neighboring center frequencies, indicated with squares, is set to be 0.4 times the peak dB-gain.

with extra frequencies is used with one iteration step to optimize the filter gains. Differences between the two designs are caused by the unequal number of bands and different bandwidths, and therefore some of the parameters must be reselected.

The third-octave design has 31 bands, whose center frequencies are given in Table 1. We use the center frequencies as well as the geometric mean frequencies between them as design frequencies, which leads to 61 design points. Thus, the size of the interaction matrix is now 61-by-31, and since it is non-square, its pseudoinverse is used in the LS design. The initial interaction matrix is designed using the same prototype gain value as the octave design, $g_p = 17$ dB.

The bandwidths for the third-octave design are defined in the same way as in the octave design by selecting a specified dB value that is achieved at the neighboring center frequencies. When using the same principle as in the octave design for calculating the bandwidths (i.e., the difference of center frequencies above and below a filter), we obtain $B_m = (\sqrt[3]{2} - 1/\sqrt[3]{2})\omega_{c,m} \approx 0.4662\omega_{c,m}$. Due to the filter asymmetry, the bandwidths of the six uppermost filters are tuned by hand, resulting in the values presented in Table 1. The effect of the manual adjustments are also seen in Fig. 8, where the left sides of the six last filters now cross the boxes at the lower neighboring center frequencies.

The largest difference between the octave and the third-octave design is found in the selection of the parameter c . Initially the value $c = 0.3$ was tested, but this resulted in too narrow filters and large approximation errors. The EQ is unable to create a flat response when the filters are too narrow, since the overall response

droops between the command points. This is shown in Fig. 9(a): when all command gains are set to +12 dB, the error exceeds 1 dB at high frequencies. Figure 9(c) shows that the same can happen in the middle frequencies with certain command gain settings.

To improve the behavior of the third-octave EQ, different values of c were tested. Additionally, a minor modification needed to be applied to the error criterion with respect to the octave design. For the third-octave design, the error is not evaluated at the intermediate points between the center frequencies, although those points are accounted for in the design. Even though the magnitude response of the EQ varies smoothly from one command point to another the approximation error exceeds 1 dB in the narrow and steep transition bands. As the transition bands are very narrow, such minor undulations are not expected to be perceivable.

Figure 10 shows the effect of parameter c on the maximum error in three different command gain settings. A suitable c parameter range for the third-octave design, where the maximum error of all three test cases remains below 1 dB, is observed to be 0.38–0.4. In this work, $c = 0.4$ is used. The improvements achieved by adjusting c to 0.4 are shown in Figs. 9(b) and in 9(d), where the approximation errors is now smaller than 1 dB and the desired accuracy is thus achieved.

Finally, a non-extreme third-octave EQ design example, taken from [12], is presented in Fig. 11(a). This command gain setting leads to a varied target curve, which the proposed design matches well, confirmed by the error curve shown in Fig. 11(b). In the plateaus, the error has been evaluated at 16 frequency points between each neighboring command points.

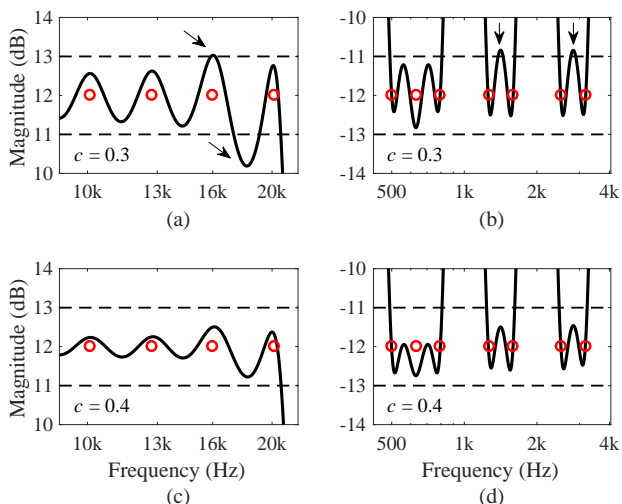


Figure 9: Effect of the value of c on the magnitude response. For (a) and (c), all the command gains are at 12 dB, and for (b) and (d), the command gains are at ± 12 dB: the target seen in Fig. 2(a) repeats itself until the 31 target points are filled. The horizontal dashed lines indicate the ± 1 -dB error tolerances and the arrows show the points where the error exceeds the 1-dB limit. The error is reduced, when the value of c is changed from 0.3 to 0.4.

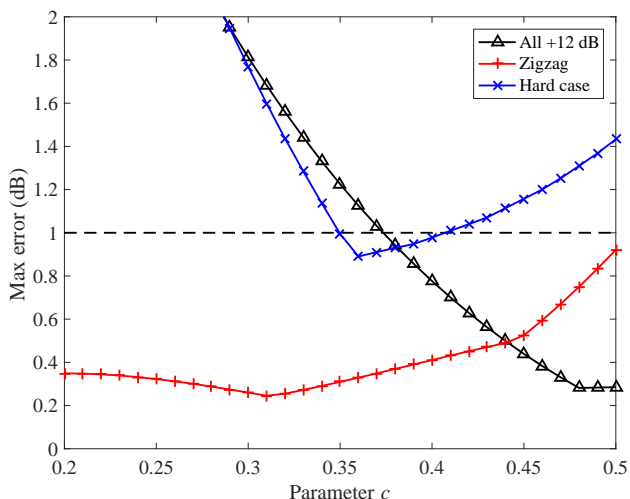


Figure 10: Effect of the parameter c on the maximum error using three different command gain settings. The hard setting is shown in Fig. 12(a).

5.1. Comparison With a Previous Accurate Method

In this section, the proposed third-octave design is compared with another graphic EQ, which, to our knowledge, is currently the most accurate, i.e., the high-precision parallel graphic EQ (PGE) [12]. It comprises twice as many second-order filter sections as there are bands and has a maximum approximation error of less than 1 dB at all tested command gain configurations. However, it is difficult to design, since a high-resolution interpolation of the target magnitude response is required as well also a phase response estimation [29].

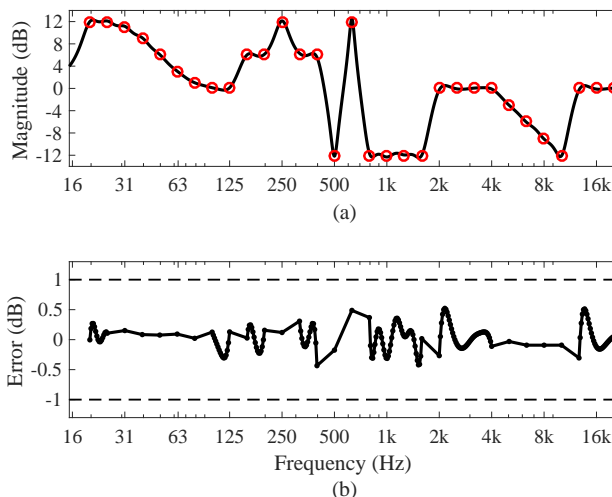


Figure 11: Third-octave EQ example showing varying command gains: (a) the complete response of the EQ and (b) the error, as defined for the third-octave design in Sec. 5. The dots illustrate the frequency points where the error has been evaluated.

Table 2 compares the accuracy of the two EQs with different command gain settings. We are interested in the maximum error that is determined by the guidelines shown in Fig. 1 apart from using the intermediate frequency points as explained in the previous section. The first test case is a zigzag setting in which the command gains alternate between ± 12 dB that reveals the EQ’s ability to create steep transitions. As is seen in Fig. 12(a) and (b), the proposed design and the PGE produce very similar responses everywhere except at very low frequencies below the first command point, and they both stay within ± 1 dB of the targets. However, when looking at the maximum error, the proposed method is slightly better with an approximately 0.2-dB smaller error.

The responses of the second test case are shown in Figs. 12(c) and (d). Here too the command gains vary between ± 12 dB, but there are also flat regions between the steep transitions. The gain setting is inspired by the ones seen in Fig. 2. However, in the case of third-octave filters we could not test all the hard binary settings as in the octave version, because of the huge number of combinations (2^{31} compared to 2^{10}). Instead, some combinations that we thought were hard were tested, and we ended up using the following demanding command gain configuration: $\mathbf{t} = [12 -12 12 12 -12 12 -12 -12 -12 12 12 -12 12 -12 12 12 -12 12 12 -12 12 12 -12 12 12 -12 12 12 -12 12 12 -12 12 12]^T$. The two methods again produce similar responses, as seen by comparing Figs. 12(c) and (d). When investigating the maximum error, we see that the PGE is slightly better, but that both methods stay within ± 1 dB of the target.

Table 3 lists the number of operations during real-time filter-

Table 2: Maximum error of two third-octave graphic EQs in two test target settings. The best result in each case is highlighted.

Case	PGE	Proposed
Zigzag	0.65 dB	0.41 dB
Hard case	0.66 dB	0.98 dB

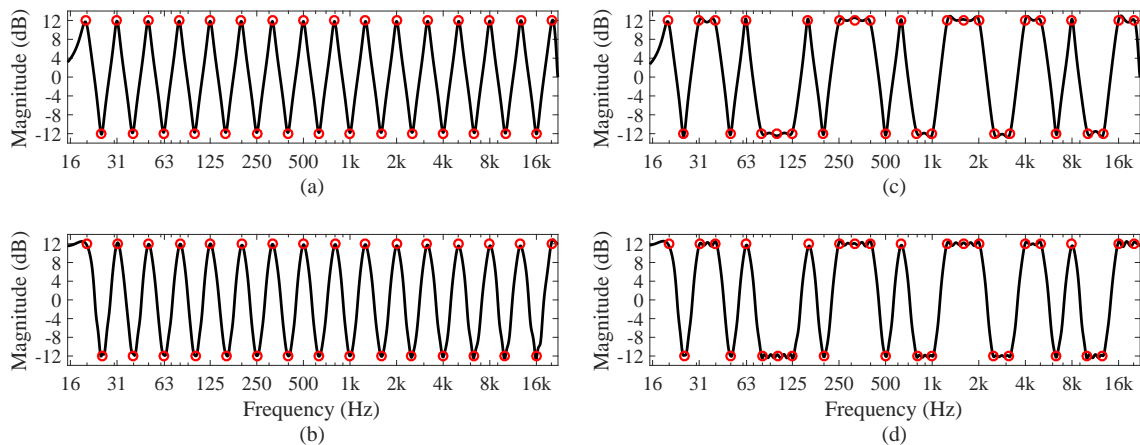


Figure 12: Magnitude response of (a) the proposed design and (b) the PGE with zigzag (± 12 dB) command settings and (c) the proposed design and (d) the PGE with hard command gain settings (± 12 dB) inspired by the targets in Fig. 2.

ing for the PGE and the proposed methods. As is seen, the proposed method is approximately 44% more efficient. This advantage mainly comes from using one biquad filter per band rather than the two per band in the PGE. Even though the PGE uses an optimized structure by having one fewer numerator coefficient compared to the traditional second-order filter [12], the larger number of filter sections negates that advantage.

Additionally, we compared another computational aspect of the graphic EQ design, namely the parameter computing time when a command gain is changed. The update times were calculated in MATLAB as an average of 1000 updates using random values between ± 12 dB as command gains. The Internet connection and all other programs were shut down so as not to affect the computation.

The average time for the command gain update was 24 ms for the PGE method and 6.0 ms for the proposed method. This implies that the proposed method is 75% faster than the PGE in updating its parameters. The proposed method requires linear interpolation between the command gains, a matrix inversion, and large matrix multiplications, which increase its update time. However, due to the computation of the high-resolution target magnitude and phase responses and a pseudoinverse of a large matrix, the PGE requires much more time to update its parameters.

In summary, the proposed method is approximately equally accurate as the PGE, but requires fewer operations per output sample and is faster in command gain updating, making it the superior design.

6. CONCLUSION AND FUTURE WORK

This paper reviewed the methods and the target response definition for graphic EQ design, proposed a methodology for testing graphic

Table 3: Comparison of the operation count in third-octave EQs.

Operations	PGE	Proposed
Additions	248	124
Multiplications	248	155
Total	496	279

EQs, and expanded a previously proposed accurate graphic EQ to the third-octave equalization problem. In the case of a cascade octave graphic EQ with low-order band filters, one alternative is to evaluate the error at intermediate points between the command points in addition to the command points themselves. This is enough to guarantee a monotonous transition between the bands, since large deviations between bands are impossible using second-order IIR filters having a restricted bandwidth. In addition, some hard command gain settings were presented that can be used to test graphic EQ designs. The largest errors were observed when all command gains were at the extreme values, usually at ± 12 dB.

Finally, a previously proposed accurate graphic EQ design was expanded to the third-octave case. The design method uses one second-order IIR filter per band. The interaction between the different band filters is optimized at the band center frequencies and at one extra point between each center frequency with the help of an interaction matrix. With one iteration step in the interaction matrix design, the method achieves 1-dB accuracy and thus is applicable to high-quality audio.

The new third-octave design was compared with a previously proposed parallel graphic EQ, which, to our knowledge, was the state-of-the-art graphic EQ prior to this work. The new method achieves approximately the same accuracy but requires fewer operations per output sample and is faster to design. The proposed method is thus currently the best graphic EQ design. The relevant MATLAB code is available online [33].

A remaining research challenge is to simplify the EQ design so that sufficient accuracy is achieved without an iteration step. Possible approaches to this end are the determination of data- or frequency-dependent c and g_p parameters. This would lead to computational benefits, since the interaction matrix and its pseudoinverse would not have to be calculated with each command gain change. Furthermore, the cascade EQ could be converted into a parallel form in order to reap benefits in the filter implementation.

7. ACKNOWLEDGMENT

The authors would like to thank Luis Costa for proofreading this paper.

8. REFERENCES

- [1] V. Välimäki and J. D. Reiss, “All about audio equalization: Solutions and frontiers,” *Appl. Sci.*, vol. 6, no. 129/5, pp. 1–46, May 2016.
- [2] D. A. Bohn, “Operator adjustable equalizers: An overview,” in *Proc. Audio Eng. Soc. 6th Int. Conf. Sound Reinforcement*, Nashville, TN, USA, May 1988, pp. 369–381.
- [3] Y. Hirata, “Digitalization of conventional analog filters for recording use,” *J. Audio Eng. Soc.*, vol. 29, no. 5, pp. 333–337, May 1981.
- [4] S. Takahashi, H. Kameda, Y. Tanaka, H. Miyazaki, T. Chikashige, and M. Furukawa, “Graphic equalizer with microprocessor,” *J. Audio Eng. Soc.*, vol. 31, no. 1/2, pp. 25–28, Jan.-Feb. 1983.
- [5] Motorola Inc., “Digital stereo 10-band graphic equalizer using the DSP56001,” 1988, Application note.
- [6] S. Stasis, R. Stables, and J. Hockman, “Semantically controlled adaptive equalisation in reduced dimensionality parameter space,” *Appl. Sci.*, vol. 6, no. 116/4, pp. 1–19, Apr. 2016.
- [7] J. Rämö, V. Välimäki, and M. Tikander, “Perceptual headphone equalization for mitigation of ambient noise,” in *Proc. IEEE Int. Conf. Acoust. Speech Signal Process. (ICASSP)*, Vancouver, BC, Canada, May 2013, pp. 724–728.
- [8] F. Vidal Wagner and V. Välimäki, “Automatic calibration and equalization of a line array system,” in *Proc. Int. Conf. Digital Audio Effects (DAFx-15)*, Trondheim, Norway, Nov. 2015, pp. 123–130.
- [9] D. Griesinger, “Accurate timbre and frontal localization without head tracking through individual eardrum equalization of headphones,” in *Proc. Audio Eng. Soc. 141st Conv.*, Los Angeles, CA, USA, Sept. 2016.
- [10] J. Liski, V. Välimäki, S. Vesa, and R. Väänänen, “Real-time adaptive equalization for headphone listening,” in *Proc. 25th European Signal Process. Conf. (EUSIPCO-17)*, Kos, Greece, Aug. 2017.
- [11] V. Välimäki and J. Liski, “Accurate cascade graphic equalizer,” *IEEE Signal Process. Lett.*, vol. 24, no. 2, pp. 176–180, Feb. 2017.
- [12] J. Rämö, V. Välimäki, and B. Bank, “High-precision parallel graphic equalizer,” *IEEE/ACM Trans. Audio Speech Lang. Process.*, vol. 22, no. 12, pp. 1894–1904, Dec. 2014.
- [13] R. J. Oliver and J.-M. Jot, “Efficient multi-band digital audio graphic equalizer with accurate frequency response control,” in *Proc. Audio Eng. Soc. 139th Conv.*, New York, NY, USA, Oct. 2015.
- [14] A. T. Johnson, Jr., “Magnitude equalization using digital filters,” *IEEE Trans. Circ. Theory*, vol. 20, no. 3, pp. 308–311, May 1973.
- [15] M. Waters, M. Sandler, and A. C. Davies, “Low-order FIR filters for audio equalization,” in *Proc. Audio Eng. Soc. 91st Conv.*, New York, NY, USA, Oct. 1991.
- [16] J. A. Henriquez, T. E. Riemer, and R. E. Trahan, Jr., “A phase-linear audio equalizer: Design and implementation,” *J. Audio Eng. Soc.*, vol. 38, no. 9, pp. 653–666, Sept. 1990.
- [17] R. Väänänen and J. Hiipakka, “Efficient audio equalization using multirate processing,” *J. Audio Eng. Soc.*, vol. 56, no. 4, pp. 255–266, Apr. 2008.
- [18] J. Siiskonen, “Graphic equalization using frequency-warped digital filters,” M.Sc. thesis, Aalto University, Espoo, Finland, Aug. 2016.
- [19] R. A. Greiner and M. Schoessow, “Design aspects of graphic equalizers,” *J. Audio Eng. Soc.*, vol. 31, no. 6, pp. 394–407, June 1983.
- [20] S. Tassart, “Graphical equalization using interpolated filter banks,” *J. Audio Eng. Soc.*, vol. 61, no. 5, pp. 263–279, May 2013.
- [21] Z. Chen, G. S. Geng, F. L. Yin, and J. Hao, “A pre-distortion based design method for digital audio graphic equalizer,” *Digital Signal Process.*, vol. 25, pp. 296–302, Feb. 2014.
- [22] P. A. Regalia and S. K. Mitra, “Tunable digital frequency response equalization filters,” *IEEE Trans. Acoust. Speech Signal Process.*, vol. 35, no. 1, pp. 118–120, Jan. 1987.
- [23] M. Holters and U. Zölzer, “Graphic equalizer design using higher-order recursive filters,” in *Proc. Int. Conf. Digital Audio Effects*, Montreal, Canada, Sept. 2006, pp. 37–40.
- [24] J. Rämö and V. Välimäki, “Optimizing a high-order graphic equalizer for audio processing,” *IEEE Signal Process. Lett.*, vol. 21, no. 3, pp. 301–305, Mar. 2014.
- [25] R. Bristow-Johnson, “The equivalence of various methods of computing biquad coefficients for audio parametric equalizers,” in *Proc. Audio Eng. Soc. 97th Conv.*, San Francisco, CA, USA, Nov. 1994.
- [26] W. Chen, “Performance of cascade and parallel IIR filters,” *J. Audio Eng. Soc.*, vol. 44, no. 3, pp. 148–158, Mar. 1996.
- [27] R. Miller, “Equalization methods with true response using discrete filters,” in *Proc. Audio Eng. Soc. 116th Conv.*, Berlin, Germany, May 2004.
- [28] D. McGrath, J. Baird, and B. Jackson, “Raised cosine equalization utilizing log scale filter synthesis,” in *Proc. Audio Eng. Soc. 117th Conv.*, San Francisco, CA, USA, Oct. 2004.
- [29] J. A. Belloch and V. Välimäki, “Efficient target response interpolation for a graphic equalizer,” in *Proc. IEEE Int. Conf. Acoust. Speech Signal Process. (ICASSP)*, Shanghai, China, Mar. 2016, pp. 564–568.
- [30] J. S. Abel and D. P. Berners, “Filter design using second-order peaking and shelving sections,” in *Proc. Int. Computer Music Conf.*, Miami, FL, USA, Nov. 2004.
- [31] S. J. Orfanidis, *Introduction to Signal Processing*, Rutgers Univ., Piscataway, NJ, USA, 2010.
- [32] L. B. Jackson, *Digital Filters and Signal Processing*, Kluwer, Norwell, MA, USA, 2nd edition, 1989.
- [33] J. Liski and V. Välimäki, “Companion page to The Quest for the Best Graphic Equalizer [Online],” <http://research.spa.aalto.fi/publications/papers/dafx17-geq/>, 2017, [accessed Jun. 21, 2017].